$$\beta_0 = \frac{1+(R_x/R_z)\cos 2\theta}{[((R_x/R_z)\sin 2\theta)^2+(1+(R_x/R_z)\cos 2\theta)^2]^{\frac{1}{2}}} \cdot \gamma_c/2$$
$$= G\,.\,\gamma_c/2\,, \qquad (7)$$

from which

$$(\gamma_R)_{\min} = |2\gamma_\lambda + \gamma_x + \gamma_c[G(1+(R_x/R_z)\cos 2\theta) + (1-G^2)^{\frac{1}{2}}(R_x/R_z)\sin 2\theta]|\,. \qquad (8)$$

Equation (8) may then replace (D.10) of the previous paper. For $2\theta \rightarrow 0°$ this expression reduces to (D.11). For $R_x = R_z$ we note that $G = \cos\theta$, and (8) becomes

$$(\gamma_R)_{\min} = |2\gamma_\lambda + \gamma_x + 2\gamma_c \cos\theta|\,, \qquad (9)$$

the last term of which is Burbank's result.

The effect of the revision of equations (D.9) and (D.10) is actually very small. Thus in Fig. 34 of the previous paper the end-points of the curves ($2\theta = 0°$ and 180°) are unchanged; only at intermediate points they now rise more quickly with increasing 2θ. For $\gamma_m = 0°$, $\gamma_x = 0.70°$, and $\gamma_c = 0{\cdot}1°$ the maximum change is only 5%, while for small mosaic crystals the change is negligible. Attention is also drawn to the various practical factors which may necessitate aperture widths somewhat in excess of the minimal values specified by (3) and (9) (Alexander & Smith, 1962; Alexander & Smith, 1963).

References

Alexander, L. E. & Smith, G. S. (1962). *Acta Cryst.* **15**, 983.

Alexander, L. E. & Smith, G. S. (1963). *Acta Cryst.* **16**, A 152.

Burbank, R. D. (1962). Unpublished manuscript.

Ladell, J. & Spielberg, N, (1963). *Acta Cryst.* **16**, 1057.

Acta Cryst. (1964). **17**, 448

Refinement of an iron chromium boride with the Mn_4B structure.

By Bruce E. Brown and D. J. Beerntsen, *Materials Research, Allis-Chalmers Mfg. Company, Milwaukee* 1, *Wisconsin, U.S.A.*

(*Received* 1 *May* 1963 *and in revised form* 19 *July* 1963)

Introduction

Several transition metal borides having the Mn_4B structure have been prepared in this laboratory as part of a study of the boride phases appearing in boron-containing chromium steels. Similar phases were studied by Andersson & Kiessling (1950), who reported an orthorhombic Cr_2B phase with space group *Abmm* or *Abm*2. Bertaut & Blum (1953) found the $CuAl_2$ type structure for Cr_2B but also found the Mn_4B structure at Cr_4B. Aronsson & Aselius (1958) prepared Cr_2B with the Mn_4B structure, analogous to the material prepared in connection with the present project, and first reported that significant amounts of chromium could be replaced by iron. Beerntsen & Brown (to be published) found by quantitative extraction and extract analysis that over half of the chromium could be replaced by iron. Other variations of the Mn_4B structure attempted were $(Cr,Mn)_2B$, $(Cr,Co)_2B$, $(Cr,Ni)_2B$, and $(Cr,V)_2B$. Only with manganese and cobalt were significant solubilities observed in Cr_2B. Complete solubility might be expected only between Cr_2B and Mn_4B (Mn_2B has the $CuAl_2$ structure) since none of the borides of vanadium, cobalt and nickel have the Mn_4B structure. Powder X-ray photographs of the manganese sample, CrMnB, can be interpreted on the basis of a single phase with the Mn_4B structure. It was estimated that about one quarter of the chromium could be replaced by Co in Cr_2B. The chromium took all the boron from the nickel preparation to yield CrB and free nickel. In the vanadium sample, the predominant product was V_3B_2 in a smaller cell than when pure, apparently because of having dissolved significant amounts of chromium.

Crystal preparation

The crystals for X-ray work were prepared by vacuum melting (melting point about 1450 °C) equimolar amounts of chromium, iron, and boron in a zirconia crucible. Ten minutes after melting occurred, the temperature was lowered to about 100 °C below the melting point for 15 minutes and was then lowered to room temperature by furnace cooling. The composition of the well-developed crystals at the bottom of the 30 g ingot was 51·0% iron, 38·6% chromium and 8·1% boron giving a formula of $Fe_{1{\cdot}1}Cr_{0{\cdot}9}B_{0{\cdot}9}$ assuming $Fe + Cr = 2{\cdot}0$. The orthorhombic cell dimensions from precession photographs were

$$a = 14{\cdot}57,\ b = 7{\cdot}32,\ c = 4{\cdot}22\ \text{Å}\,.$$

Refinement

The Mn_4B structure (Kiessling, 1950) is in space group *Fddd* with 32 metal atoms on two sets of special positions, 16(e) and 16(f). The boron atoms are on a second set of 16(e) positions. All boron sites are occupied in FeCrB as in Cr_2B in contrast to Mn_4B where eight boron atoms must be distributed among sixteen sites. Ordering of iron and chromium was tested by means of a least-squares refinement.

X-ray intensity data were gathered by a peak intensity method from photographs made by the Weissenberg technique. Three levels about the a axis and six levels about the c axis were measured, giving a total of 335 separate reflections. A crystal was made into a sphere with a Bond sphere grinder (Bond, 1951), and absorption corrections were made from tables for spherical crystals (Evans & Ekstein, 1952). The intensities were also corrected for Lorentz-polarization, α_1, α_2 separation, and upper level Weissenberg extension contraction effects (Phillips, 1956).

In space group *Fddd* the y and z parameters are fixed for position (e) and the x and z parameters are fixed for position (f). Only three positional parameters are variable, one per atom of the asymmetric unit. Ordering can occur such that: (1) iron is on (e), chromium is on (*f*); (2) chromium is on (*e*), iron is on (*f*); or (3) iron and chromium are mixed on (*e*) and (*f*) in a regular way. In case (3) symmetry will be changed from *Fddd*.

Fddd was considered to be essentially correct, as indicated by systematic absences, but we refined the structure using six variable position parameters and six temperature factors rather than the three of each required. This amounted to refining the structure utilizing only the symmetry centers but fixing y and z for (*e*) positions and x and z for (*f*) positions as required by *Fddd*. No significant departures from *Fddd* in positional parameters or temperature factors were encountered in using this procedure (Table 1). Refinement was carried out with the Busing–Levy (1959) least-squares program for the IBM 704 with the use of the scattering factors for iron of Veenendaal, MacGillavry, Stam, Potters & Romgens (1959), for chromium of Berghuis, Haanappel, Potters, Loopstra, MacGillavry & Veenendaal (1955), and for boron of Ibers (1957). The R value from the refined structure is 12·6%. The final parameters are given in Table 1.

Table 1. *Positional and temperature factor parameters with standard deviations*

M(*e*) denotes metal atoms on (*e*) special positions, M(*f*) denotes metal atoms on (*f*) special positions, and B(*e*) denotes boron atoms on (*e*) special positions. The fixed parameters are for the (*e*) positions $y=z=\frac{1}{8}$ and for the (*f*) positions $x=z=\frac{1}{8}$. Origin at $\bar{1}$

	X				
	Observed using symm. centers only	Adjusted to *Fddd* using $x=\frac{1}{4}-x$	$\sigma(X)$	B	$\sigma(B)$
M(*e*)	0·2075	0·2070	0·0003	0·139	0·026
	0·0435	0·0430	0·0003	0·180	0·026
B(*e*)	0·498	0·500	0·004	0·85	0·42
	0·755	0·750	0·004	1·32	0·41

	Y				
	Observed using symm. centers only	Adjusted to *Fddd* using $y=\frac{1}{4}-y$	$\sigma(Y)$	B	$\sigma(B)$
M(*f*)	0·4572	0·4571	0·0004	0·200	0·027
	0·7930	0·7929	0·0004	0·175	0·027

The standard deviation of the electron density was calculated according to (Cruickshank, 1949):

$$\sigma(\varrho)=\frac{1}{V}\Big[\sum_h\sum_k\sum_l(F^2)\Big]^{\frac{1}{2}}$$

and includes a correction for recording only from about 50% of the space in the reflecting sphere. The value of 1·0 e.Å^{-3} derived from this calculation is proportional to about 0·15 e. in the volume of an iron or chromium peak. If a difference of three standard deviations is significant then differences of the order of 0·45 e. or about a 20% ordering of iron and chromium is detectable. No significant differences in electron densities were present between any of the metal positions on a three-dimensional difference Fourier map and a disordered condition is indicated.

Interatomic distances are catalogued in Table 2 along with standard deviations of the bond lengths. The standard deviation of bonds between equivalent atoms was calculated from the relation $\sigma_{12}=2\sigma_1$ because their variances are dependent. Deviations of bonds between non-equivalent atoms are found from the relation $\sigma_{12}^2=\sigma_1^2+\sigma_2^2$. All of these atoms are on special positions and are pinned so that a given atom can vary only in one dimension. Therefore the components of the atomic standard deviations in the direction of the bond

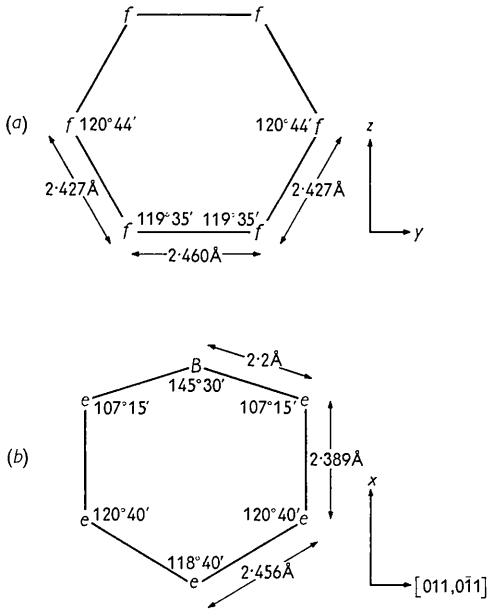

Fig. 1. Geometry of interatomic distances among (*e*) and (*f*) positions.

Table 2. *List of interbond distances and angles, with standard deviations*

Numbers in parentheses denote distribution of distances among near neighbors of the atom in the leftmost column

	No. of near neighbors	M(*e*)	Boron	M(*f*)
M(*e*)	15	2·456 ± 0·004 Å (2) 2·389 ± 0·008 (1)	2·195 ± 0·016 Å (2) 2·210 ± 0·017 (2)	2·734 ± 0·004 Å (2) 2·719 ± 0·002 (4) 2·708 ± 0·003 (2)
Boron	10	2·195 ± 0·016 (2) 2·210 ± 0·017 (2)	2·113 (2)	2·164 ± 0·05 (2) 2·222 ± 0·05 (2)
M(*f*)	15	2·734 ± 0·004 (2) 2·719 ± 0·002 (4) 2·708 ± 0·003 (2)	2·164 ± 0·05 (2) 2·222 ± 0·05 (2)	2·460 ± 0·006 (1) 2·427 ± 0·003 (2)

must be considered in computing the bond length standard deviation. The description of the disposition of these distances with respect to interatomic angles follows.

The M(*f*) atoms are located at the vertices of hexagons whose plane is parallel to (100) (Fig. 1(*a*)). The longer 2·460 Å bonds are directed parallel to *y* and the 2·427 Å bonds are perpendicular to (011) and (01$\bar{1}$). Angles in the hexagon deviate slightly from 120° so that the four angles formed by the intersection of a long and a short M(*f*)–M(*f*) bond are equal to 119° 37′ and the two angles formed by the intersection of two shorter M(*f*)–M(*f*) bonds are equal to 120° 46′.

The M(*e*) atoms are located on hexagons parallel to (011) and (01$\bar{1}$) which include one boron atom (Fig. 1(*b*)). Of the six sides of the hexagon two are the shorter M(*e*)–M(*e*) 2·389 Å bonds parallel to *x*, two are the longer M(*e*)–M(*e*) 2·456 Å bonds, perpendicular to (131) and ($\bar{1}$31) or (13$\bar{1}$) and ($\bar{1}$3$\bar{1}$) and two are the 2·2 Å M(*e*)–B bonds. Of the six angles two are formed by intersection of a long and a short M(*e*)–M(*e*) and equal 120° 40′, two are formed by intersection of a short M(*e*) bond and an M(*e*)–B bond and equal 107° 15′, one is formed by intersection of two longer M(*e*)–M(*e*) bonds and equals 118° 40′, and one is formed by intersection of two M(*e*)–B bonds and equals 145° 30′.

All M(*e*) to M(*f*) distances can be depicted as sides of a distorted tetrahedron as originally described by Kiessling (1950). All of these distances are long (greater than 2·7 Å), relative to the M(*e*)–M(*e*) and M(*f*)–M(*f*) distances. The articulation of the longer M(*f*)–M(*e*) distances with the shorter M(*e*)–M(*e*) and M(*f*)–M(*f*) distances results in distorted tetrahedra so that the triangular faces of these tetrahedra are isosceles rather than equilateral, with two larger angles of about 64° and one smaller one of about 52°.

The boron atoms, as also noted by Kiessling (1950), lie in strings perpendicular to (031) or (03$\bar{1}$) alternating at intervals of $\frac{1}{4}a$ with a boron–boron distance of 2·1 Å.

References

Andersson, L. H. & Kiessling, R. (1950). *Acta Chem. Scand.* **4**, 160.
Aronsson, B. & Aselius, J. (1958). *Acta Chem. Scand.* **12**, 1476.
Berghuis, J., Haanappel, IJ. M., Potters, M., Loopstra, B. O., MacGillavry, C. H. & Veenendaal, A. L. (1955). *Acta Cryst.* **8**, 478.
Bertaut, F. & Blum, P. (1953). *C. r. Acad. Sci. Paris*, **236**, 1055.
Bond, W. L. (1951). *Rev. Sci. Instrum.* **22**, 344.
Busing, W. & Levy, H. A. (1959). Oak Ridge National Laboratory, Central Files, No. 59-4-37.
Cruickshank, D. W. J. (1949). *Acta Cryst.* **2**, 65.
Evans, H. T. & Ekstein, M. G. (1952). *Acta Cryst.* **5**, 540.
Ibers, J. A. (1957). *Acta Cryst.* **10**, 86.
Kiessling, R. (1950). *Acta Chem. Scand.* **4**, 146.
Phillips, D. C. (1956). *Acta Cryst.* **9**, 819.
Veenendaal, A. L., MacGillavry, C. H., Stam, B., Potters, M. & Romgens, M. J. H. (1959). *Acta Cryst.* **12**, 242.

Acta Cryst. (1964). **17**, 450

The structure of (Ti, Re)Si$_2$.

By W. J. Duffin, E. Parthé and J. T. Norton, *Metallurgy Department, Massachusetts Institute of Technology, Cambridge, Massachusetts, U.S.A.* and *Department of Metallurgical Engineering, University of Pennsylvania, Philadelphia, Pennsylvania, U.S.A.*

(*Received* 22 *July* 1963)

Nearly all transition metals form disilicides. Of special interest are the disilicides with metals of the fourth to sixth group of the periodic system. They crystallize with three different crystal structure types which are geometrically related. They can be described as different stacking variations of graphite-like, metal-centered Si nets. The three types are:

*C*54 or $TiSi_2$ type: A 4-layer stacking type, which occurs with $TiSi_2$.

*C*40 or $CrSi_2$ type: A 3-layer stacking type, which has been reported for VSi_2, $NbSi_2$, $TaSi_2$, $CrSi_2$.

*C*11 or $MoSi_2$ type: A 2-layer stacking type, which has been found with $MoSi_2$, WSi_2 and $ReSi_2$.

These disilicide types and their mutual solubility have been studied extensively over the last ten years by Nowotny and his co-workers (Nowotny, 1963). It was found that the occurrence of these structure types is influenced by a valence electron factor and it is possible to change the structure type by replacing part of the metal and non-metal component with other elements having more or fewer valence electrons.

No investigations have been made before with $ReSi_2$. It was of interest to investigate how the rules developed for the 4th, 5th and 6th group disilicides would apply to $ReSi_2$. Therefore, a study of the phases and their

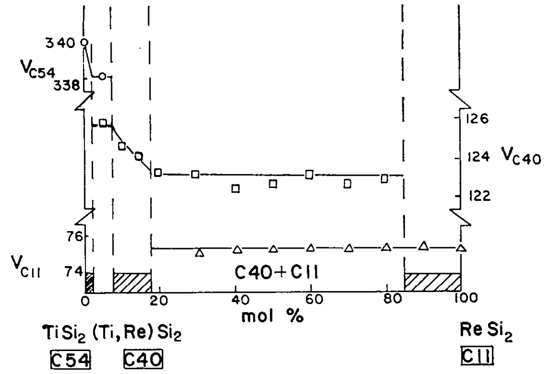

Fig. 1. Unit-cell volume (Å^3) of the phases in the pseudobinary system $TiSi_2$–$ReSi_2$ at 1300 °C.